Received: 15 June 2020 | Revised: 17 August 2020 | Accepted: 17 August 2020

DOI: 10.1002/pol.20200416

ORIGINAL ARTICLE

JOURNAL OF POLYMER SCIENCE WILEY

Correlation between backbone and pyridine dynamics in poly(2-vinyl pyridine)/silica polymer nanocomposites

Eric J. Bailey[1] | **Madhusudan Tyagi**[2,3] | **Karen I. Winey**[1]

[1]Department of Materials Science and Engineering, University of Pennsylvania, Philadelphia, Pennsylvania

[2]Center for Neutron Research, National Institute of Standards and Technology, Gaithersburg, Maryland

[3]Department of Materials Science and Engineering, University of Maryland, College Park, Maryland

Correspondence
Karen I. Winey, Department of Materials Science and Engineering, University of Pennsylvania, Philadelphia, PA 19104.
Email: winey@seas.upenn.edu

Funding information
Basic Energy Sciences, Grant/Award Number: SC0016421; Directorate for Education and Human Resources, Grant/Award Number: DGE-1321851; Division of Chemical, Bioengineering, Environmental, and Transport Systems, Grant/Award Number: 1706014; Division of Materials Research, Grant/Award Numbers: 1508249, 11-20901

Abstract

Polymer segmental dynamics in polymer nanocomposites (PNCs) can be significantly perturbed from bulk and underlie macroscopic mechanical and transport properties, but fundamental studies are necessary to build correlations between dynamics and properties. To elucidate a mechanistic description of this perturbation and isolate different molecular motions, we present quasi-elastic neutron scattering (QENS) measurements on PNCs with attractive interactions comprised of colloidal silica nanoparticles (NPs) uniformly dispersed in poly(2-vinyl pyridine) (P2VP) with and without backbone deuteration. Measurements of fully-protonated P2VP probe the dynamics of both the polymer backbone and pyridine pendant group; whereas measurements of backbone-deuterated P2VP isolate the dynamics of only the pyridine ring. On the small length scales (~1 nm) and fast time scales (~1 ns) captured by QENS, we show that the backbone and pyridine ring dynamics are highly coupled at high temperatures and both are slowed by about 35% relative to neat polymer in 25 vol% PNCs. This observation implies that the backbone and pendant interfacial dynamics are perturbed similarly in PNCs, which further develops our fundamental understanding of microscopic properties in PNCs.

KEYWORDS

neutron scattering, polymer nanocomposites, quasi-elastic neutron scattering, segmental dynamics, segmental relaxations

1 | INTRODUCTION

Polymer nanocomposites (PNCs), comprised of nanoparticles (NPs) dispersed in a polymer matrix, have attracted significant attention in recent decades due to their superior properties relative to the bulk homopolymer.[1–3] For example, the addition of NPs to a polymer matrix can improve the mechanical properties of glassy and melt polymers[4,5] and enhance small molecule transport.[6,7] However, the microscopic origin of many of these altered macroscopic properties remains mechanistically unknown. In the specific case of mechanical and transport properties, segmental dynamics often underlie and dictate these properties in the melt. For PNCs, it is therefore advantageous to develop a fundamental understanding of the impact of NPs on different molecular motions to guide the design and development of PNC materials and optimize PNC properties.[3]

Recently, poly(2-vinyl pyridine) (P2VP) and silica (SiO_2) has emerged as a model PNC system to study materials with attractive NP-polymer interactions. In fact, several works have studied dynamics in this system at different length scales including segmental dynamics,[8–13] chain dynamics,[14] and nanoparticle dynamics.[15] For

example, broadband dielectric spectroscopy (BDS) revealed the primary structural α-relaxation near the NP surface is ~100x slower than bulk.[8,9] These slow segmental relaxations are accompanied by slight increases in the glass transition temperature (T_g) as measured by differential scanning calorimetry (DSC).[8,11,13] We recently reported quasi-elastic neutron scattering (QENS) measurements on this P2VP/SiO_2 system.[11] We showed reduced segmental mobility in PNCs relative to bulk at each temperature studied, namely ~80% slower segmental diffusion at 50 vol% NP concentration for $T >> T_g$, and that these effects were mostly independent of molecular weight.[11] We also observed a layer near the NP surface (~1 nm thick) that relaxed at timescales slower than the available temporal range, which qualitatively follows observations from a variety of techniques.[14,16,17] QENS has the additional capability to probe the spatial dependence of relaxations, unlike other strictly temporal measurements (such as BDS and temperature modulated DSC). Therefore, QENS provides valuable insights into understanding relaxation processes in various PNCs systems.[6,18–21] In P2VP/SiO_2, our previous measurements showed that the spatial dependence of the segmental relaxation time was comparable between bulk and PNCs, implying spatially similar relaxations, despite the slower average relaxation rate.[11]

Beyond the primary α-process, polymer segments can exhibit secondary relaxation such as the β-process attributed to nondiffusive relaxations or reorientations of segments or pendant groups in monomers.[3,21] In PNCs, these secondary relaxations have received less attention. In one contribution, a combined QENS, BDS, and Brillouin light scattering study of P2VP/SiO_2 observed picosecond dynamics below T_g and correlated them to changes in mechanical properties.[10] In matrix-free PNCs with either grafted or adsorbed polymer at $T < T_g$, the authors observed secondary relaxations that were faster than bulk which the authors attribute to chain packing and density fluctuations in these highly loaded PNCs.[10] This result is in direct contrast to the primary α-process which is slower than bulk in both systems.[22] This low temperature ($T \leq T_g$), decoupling between primary and secondary relaxations has been reported in bulk and confined systems.[21,23]

In this article, we present QENS measurements to further fundamentally understand the segmental dynamics and molecular motions in neat polymer and PNC melts. By measuring bulk polymer and PNCs comprised of fully-protonated P2VP and partially deuterated (backbone deuterated) d3P2VP, we aim to decouple the dynamics of the pendant group and backbone chain in polymer melts and PNCs. Partial deuteration of polymers has been successful in differentiating molecular motions and contributions to relaxations using QENS in neat polymer, polymer blends, and unique PNCs.[18,24,25] The separation of backbone and pendant motion in PNCs is critical to understanding previous measurements of various dynamics in this model PNC system and more broadly understand how polymer segments relax in the presence of NPs.

2 | EXPERIMENTAL DETAILS

P2VP (30.9 kg/mol, 1.1 PDI) and d3P2VP (33.6 kg/mol, 1.2 PDI) samples were purchased from Scientific Polymer Products and Polymer Source, respectively, and used as received. Polymer molecular weight distributions were characterized via GPC. The T_g of both polymers, as measured by DSC at a cooling rate of 5 K/min, is 370 K. Ludox AS-40 colloidal SiO_2 NPs were obtained from Sigma-Aldrich and received dispersed in water. Following previous works,[26] SiO_2 NPs were transferred to dimethylformamide (DMF). Concentrated NP solutions in water were diluted with DMF to ~50 g/L and then the solution was distilled at 130°C. DMF was added and the distillation was repeated until the H_2O content as measured by Karl Fisher titration was <0.1 wt%. The measured NP diameter (d_{NP}) was 28 ± 3 nm as characterized by small-angle X-ray scattering (SAXS), dynamic light scattering, and transmission electron microscopy.

Samples were fabricated via solution processing. P2VP and d3P2VP were dissolved in DMF (~5 wt% polymer) and for PNCs, were mixed with SiO_2/DMF solutions (~20 g/L SiO_2). Solutions were stirred continuously overnight to ensure formation of the bound polymer layer in solution, which is known to lead to good NP dispersion.[15,27] Solutions were drop cast in a hot PTFE dish (383 K) then vacuum dried at T_g + 100 K for 24 hours. Both PNC materials exhibit a slight increase in T_g (~372 K) in agreement with various calorimetry measurements.[3,8,11] For QENS measurements, at least 200 mg of polymer was encased in aluminum foil (with thickness on the order of 200 μm) and placed in cylindrical aluminum cans during measurement.

NP concentrations were measured via thermogravimetric analysis (TGA) where ~5 mg samples were heated beyond 1,100 K in platinum pans to measure the total remaining SiO_2 mass. Small-angle X-ray scattering ($0.008 < q < 0.12$ Å^{-1}) was conducted at the Multi-angle X-ray Scattering (MAXS) facility at the University of Pennsylvania to characterize the NP size in solution and dispersion in PNC films. Measurements in solution were at a SiO_2 concentration of 1 mg/mL in H_2O. QENS measurements were conducted at the high-flux backscattering spectrometer (HFBS, NG2) at the NIST Center of Neutron Research in Gaithersburg, MD.[28] Fixed window scans (FWS) and QENS measurement conditions

and parameters are reported in our previous publication.[11] Importantly, HFBS probes $0.25 < q < 1.75$ Å^{-1} and $-17 < h\upsilon < 17$ μeV (with a resolution of 0.8 μeV obtained from measurements of vanadium). Therefore, the probed molecular motions are approximately 3–25 Å and 40 ps – 2 ns. Samples were loaded at room temperature, heated above T_g under vacuum to remove any residual solvent or adsorbed water and equilibrate the sample. After cooling to 50 K, FWS were conducted at heating rates of 1 K/min to 535 K then QENS measurements were recorded at the desired temperatures with at least 10 hr of collection at each temperature. We reported a stability and degradation analysis of P2VP and this QENS experiment after measuring several temperatures (up to 550 K) in our previous publication.[11]

3 | RESULTS AND DISCUSSION

This model attractive PNC system of P2VP/SiO_2 is known to form well-dispersed mixtures due to the strong NP-polymer attraction, which forms a bound polymer layer and prevents NP–NP aggregation.[15,27] SAXS patterns that were shifted for clarity are shown in Figure 1b. Although slight differences at low q are apparent, the similarities between P2VP and d3P2VP PNCs mean both PNCs exhibit similar NP structure, regardless of deuteration. The plateau at low q and the undulations similar to NPs in solution at intermediate q indicate a lack of NP–NP aggregates in these PNC films, as expected from previously reported PNCs, including our previous work.[11,15,27] The NP concentration in both PNC films is ~25 vol% (~40 wt%), as measured by TGA in the inset of Figure 1.

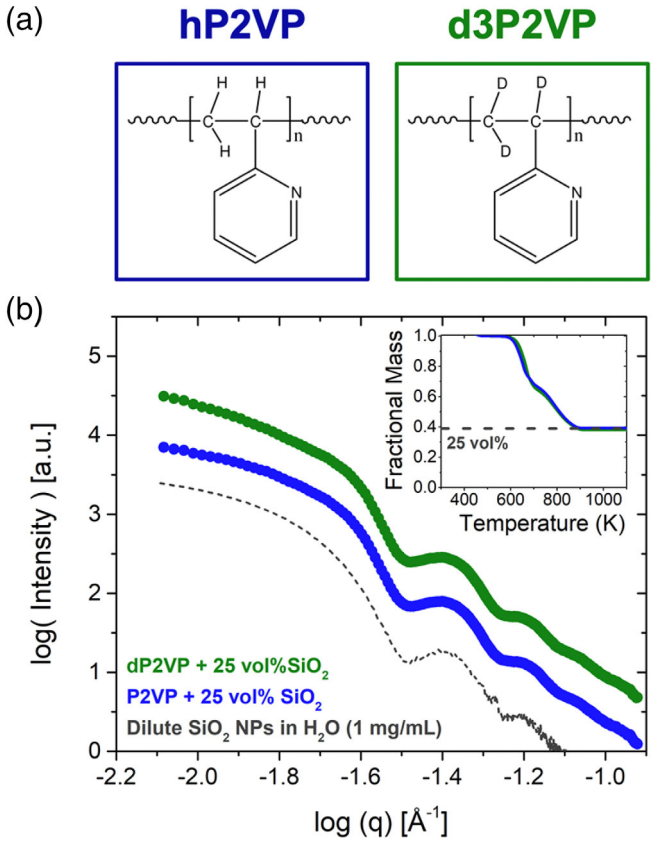

FIGURE 1 (a) Chemical structure of P2VP (blue) and d3P2VP (green), (b) SAXS of PNCs and SiO_2 NPs in solution, all shifted vertically for clarity. (inset of b) TGA measurements of PNCs showing similar NP concentrations in PNCs [Color figure can be viewed at wileyonlinelibrary.com]

While X-ray scattering probes the NPs (with a higher electron density), neutron scattering preferentially probes the polymer.[18] In particular, since the incoherent scattering cross-section (σ) for hydrogen ($\sigma_H \sim 80$ barnes) is much larger than other atoms (σ_D, σ_C, σ_{Si}, σ_O, $\sigma_N < 6$ barnes), QENS is primarily sensitive to the motion of protons in these samples.[29] Thus, deuteration of the backbone in d3P2VP/SiO_2 PNCs isolate motion of the protons in the pyridine ring while fully hydrogenated P2VP/SiO_2 PNCs reveal the combined backbone and pyridine motion. As a result, comparing measurements of d3P2VP and P2VP (Figure 1a) will identify the similarities and differences between backbone and pyridine pendant motion in neat polymer and SiO_2-based PNCs. Unfortunately, d4P2VP with a deuterated pendant pyridine group, which would isolate only backbone motion and provide further insight into the molecular motions, is difficult to synthesize and unavailable commercially.

To characterize the segmental mobility of neat P2VP, neat d3P2VP, and both PNCs over a broad temperature range, the elastic scattering intensity was monitored as a function of temperature from 50 to 535 K in a FWS. The mean-squared displacements of segments ($\langle x^2 \rangle$) shown in Figure 2 were extracted using the Debye-Waller approximation:

$$\frac{I_{elastic}}{I_0} = \exp\left(-\frac{q^2}{3}\langle x^2 \rangle\right), \quad (1)$$

where $I_{elastic}/I_0$ is the elastic scattering intensity at any given temperature normalized by the elastic scattering at T = 50 K. In practice, $\langle x^2 \rangle$ is obtained directly as the slope of $-3 \cdot \ln(\frac{I_{elastic}}{I_0})$ plotted as a function of q^2 for $q^2 < 1.22$ Å^{-2}.[11,30] This analysis assumes motions beyond the instrumental resolution produce a change in the elastic scattering that can be modeled as simple harmonic springs. We use this analysis to indicate of the average proton mobility in the sample.

At low temperatures in Figure 2a, $\langle x^2 \rangle$ is less than ~1 Å^2 which is consistent with measurements of polymer glasses since the α-relaxation process is inactive at

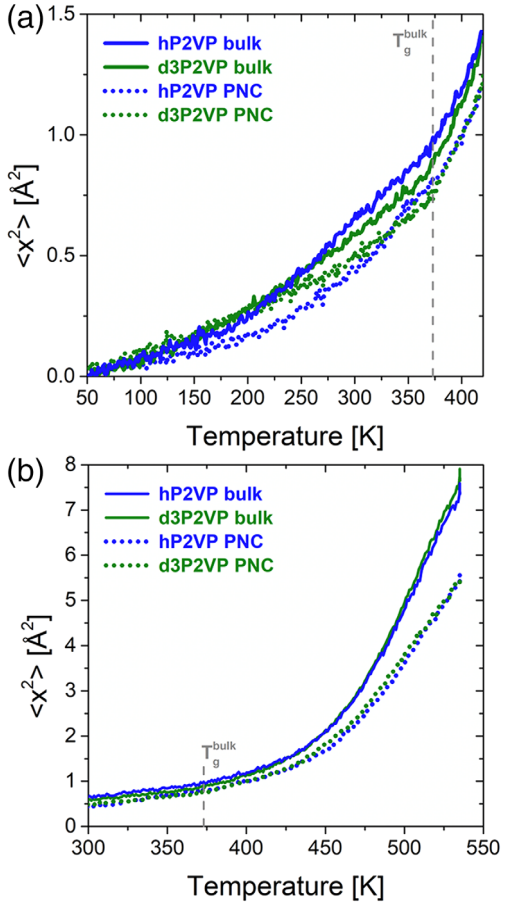

FIGURE 2 Fixed window scans of bulk polymers and PNCs with 25 vol% SiO_2, plotted as mean-squared displacements of segments ($\langle x^2 \rangle$) as a function of temperature. For clarity, (a) focuses on $\langle x^2 \rangle$ at low temperatures and (b) focuses on $\langle x^2 \rangle$ at high temperatures [Color figure can be viewed at wileyonlinelibrary.com]

$T < T_g$.[30,31] Slight differences between P2VP and d3P2VP materials are apparent in this low-temperature regime. The deuterated PNC sample appears more similar to the corresponding deuterated bulk sample than the P2VP PNC is to bulk P2VP. This is likely because the pyridine ring motion (β-process) is local enough to occur at these low temperatures,[10] even in the PNCs. Since the d3P2VP measurement is dominated by these most-mobile protons in the pyridine ring, the NPs are apparently less impactful at these temperatures. Furthermore, this implies that the backbone motion, which only contributes to the FWS in the P2VP-based materials, is slowed near the NP surface, which has been widely reported in dielectric and calorimetry studies in this temperature regime.[3,8,11] However, our measurements of d3P2VP materials show decoupled motion of the backbone and pyridine ring at these low temperatures (Figure 2a). Additional and more thorough studies of this temperature regime require full measurements of the QENS spectrum with more sensitivity to faster dynamics.

As the temperature approaches the calorimetric T_g, both PNC samples diverge from their respective bulk polymer. In Figure 2b, a sharp increase in $\langle x^2 \rangle$ is observed for $T > T_g$ in all samples due to the activation of the α-process and other segmental motions. At these higher temperatures, convergence is observed between d3P2VP and P2VP neat polymer as well as both PNCs, although d3P2VP segments may be slightly more mobile in both cases. In both P2VP and d3P2VP, the segmental mobility decreases by the addition of attractive SiO_2 NPs, in agreement with our previous QENS measurements.[11] The small differences between P2VP and d3P2VP samples in Figure 2b indicate that the mobility of the pyridine ring does not differ significantly from the backbone. This observation is in direct contrast to semiconducting P3HT[32] and PVAc melts,[23] both of which exhibit side chain dynamics decoupled from backbone dynamics in neat polymer.

To further characterize the segmental dynamics, QENS measurements were conducted at 515 and 535 K, where segments are highly mobile ($\langle x^2 \rangle > 4$ Å^2, Figure 2). As shown in the representative QENS spectra in Figure 3, all samples show significant broadening beyond the experimental resolution and the broadening in PNCs is markedly reduced from bulk. In other words, segmental dynamics are active in all samples but clearly slower in PNCs. These QENS spectra are fit with a linear combination of a delta function for the elastic scattering peak, a single Lorentzian for the segmental motion, and a linear background for background signal and secondary dynamics faster than the

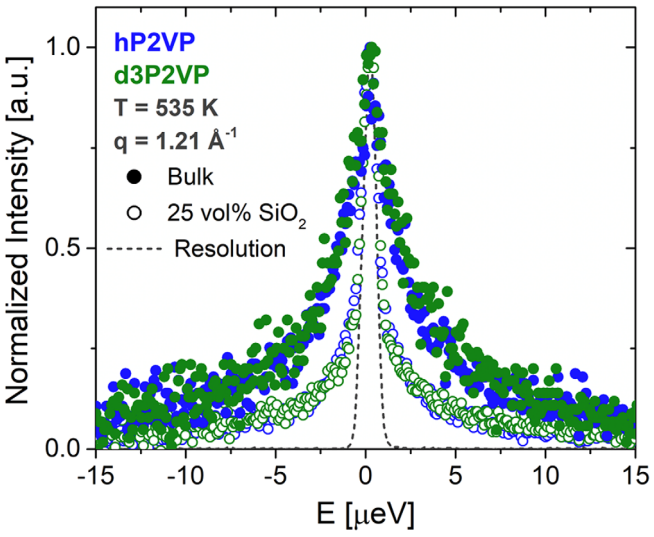

FIGURE 3 Normalized QENS spectra for bulk (solid symbols) and PNCs (open symbols) for P2VP (blue) and d3P2VP (green) samples at T = 535 K and q = 1.21 Å^{-1}. Gray line shows experimental resolution obtained from measurements of vanadium. Fits to data are presented in Supporting Information [Color figure can be viewed at wileyonlinelibrary.com]

temporal window. These functions are convoluted with experimental resolution (*Res*) obtained from measurements of bulk vanadium. Mathematically, S(q,ω) can be written as:

$$S(q,\omega)\tilde{Res}(\omega) * \{EISF(q)\cdot\delta(q) + (1-EISF(q)) \cdot L(\Gamma(q),\omega) + A(q,\omega)\}, \quad (2)$$

where L, δ, and A are Lorentzian, delta, and background functions, respectively, EISF is the elastic incoherent scattering function, Γ(q) is the half-width at half-maximum of the Lorentzian function, and * denotes a convolution. Mathematically, the Lorentzian function used to describe the dynamics can be written as:

$$L(\Gamma(q),\omega) = \pi^{-1}\frac{\Gamma(q)}{\omega^2 + \Gamma(q)^2}. \quad (3)$$

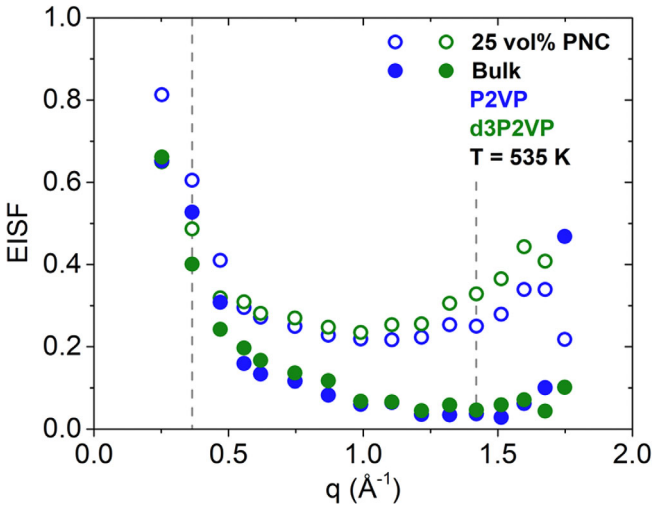

FIGURE 4 EISF for P2VP (blue) and d3P2VP (green) for bulk polymer (open circles) and PNCs (closed circles) as a function of q for data measured at T = 535 K. The data between the dashed vertical lines correspond to the region over which dynamics are analyzed [Color figure can be viewed at wileyonlinelibrary.com]

This relatively simple fitting procedure, that is, one Lorentzian used to account for the mobile species, describes the spectra well for each material system, temperature, and q, in agreement with our previous P2VP/SiO_2 measurements over extended measurement conditions.[11] Representative spectra and fits to the spectra shown in Figure 3 are provided in Figure S2 and the featureless residual plots are shown in Figure S3.

The EISF (defined in Equation (2)) characterizes the fraction of scatterers that are dynamically inactive or moving slower than the temporal resolution of the measurement and is largely independent of the model used for analysis. As shown in Figure 4 for T = 535 K, the EISF as a function of q for P2VP and d3P2VP materials are nearly indistinguishable and both PNCs consistently exhibit a larger EISF than the bulk materials. The same observations are made at T = 515 K (Figure S4). The q-dependence of the EISF for each material is similar to other polymers at T > T_g[21,33] and our previous measurements of P2VP,[11] but meticulous fitting of the data will not assist in differentiating the behavior of P2VP and d3P2VP segments.

The addition of SiO_2 NPs to a polymer matrix increases the extracted EISF, because SiO_2 scatters purely elastically at these temperatures, times, and length scales. Thus, the PNC data exhibits a larger fraction of immobile species, see Figure 4. In our previous publication[11] we used the EISF to estimate the thickness of the interphase region over which segmental motion was slowed beyond the experimental window and found a layer thickness of ~1 nm that was independent of M_w or NP concentration. The same concept is evident in this dataset, although the presence of deuterium increases the uncertainty in the extracted layer thickness. The apparent similarities between the P2VP and d3P2VP materials in Figure 4 is somewhat surprising because the backbone and pyridine ring may be expected to have different spatial relaxations which may impact the immobile fraction of scatterers as a function of q. In short, the similarities observed in Figure 4 indicate similar motion observed in both sets of samples.

To further analyze the motions within these materials, we turn to the full-width at half-maximum (FWHM) of the Lorentzian, FWHM(q) = 2Γ(q), as defined in Equation (2). The FWHM more thoroughly characterizes dynamics than the EISF because it is inversely related to the average relaxation time of the mobile protons. Figure 5a,b show the extracted FWHM as a function of q^2 for 515 K and 535 K, respectively. We report the FWHM of each sample at 515 K in Figure 5a, which may be relevant for future experiments and molecular dynamics simulations, but we refrain from further analyzing these data because all samples exhibit similar FWHM (<~4 μeV) with nonnegligible scatter. However, it can be qualitatively deduced from Figure 5a that at 515 K, the d3P2VP samples show faster dynamics than P2VP samples, especially at higher q, and both PNCs are less mobile than their bulk counterparts. In Figure 5b, systematically more broadening is observed at higher temperatures, as expected by faster dynamics.

As observed in Figure 5b at 535 K, the d3P2VP samples exhibit slightly faster dynamics than their P2VP counterparts for both neat polymers and PNCs for all q. The FWHM of each sample varies linearly with q^2,

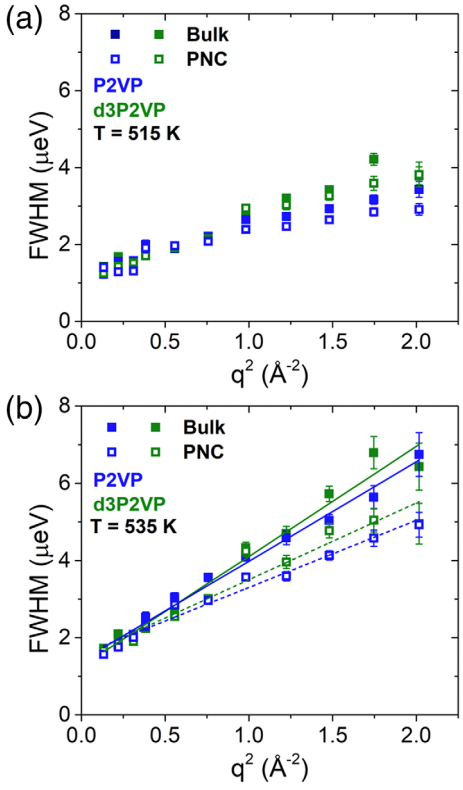

FIGURE 5 Full-width at half-maximum (FWHM) extracted from QENS spectra as a function of q^2 for P2VP (blue) and d3P2VP (green) bulk polymer (closed symbols) and PNCs (open symbols) at (a) T = 515 K and (b) T = 535 K. Lines in (b) are linear fits to data, as discussed in the text [Color figure can be viewed at wileyonlinelibrary.com]

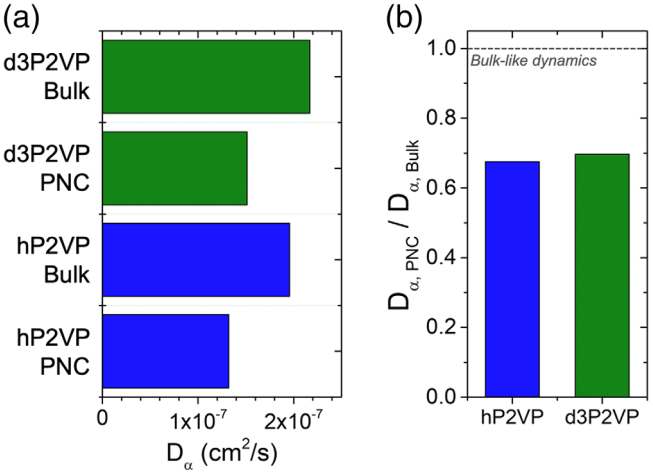

FIGURE 6 (a) Diffusion coefficients of segments in each material system at T = 535 K. (b) Diffusion coefficient of PNCs normalized by the diffusion coefficient in bulk [Color figure can be viewed at wileyonlinelibrary.com]

which indicates diffusive motion (i.e., $\tau^{-1} \sim q^2$) where the slope is related to the diffusion coefficient, D_α. This observation and analysis matches our previous report.[11] While other models can be used to describe the q-dependence,[33] we choose this relatively simple model, because it minimizes the number of fitting parameters while accurately capturing the experimental results and reveals D_α which characterizes the average rate at which segments are moving. The fits are presented with the data in Figure 5b. Interestingly, the y-intercept of each sample is similar, FWHM ~1.4 μeV. Although assigning a dynamic motion to this feature is beyond the scope of the study, we suspect it represents fast, q-independent motion dictated by protons in the pyridine ring. Although it is difficult to definitively prove, we suspect this observation is not a result of multiple scattering in part because the calculated neutron transmission through each sample is more than 90%.

The fit results of D_α from data in Figure 5b (T = 535 K) are shown in Figure 6. Considering the bulk polymers first, D_α is only ~12% faster in d3P2VP as compared to P2VP. This implies the motion of the pyridine ring is slightly faster than the motion of the backbone and that they are highly coupled at 535 K. The observation is consistent with expectations that pendant groups are generally more mobile than the chain backbone, but that the motions are spatially and temporally related at high temperatures ($T >> T_g$). In both PNCs, D_α is reduced relative to their bulk counterparts. In fact, by plotting the normalized segmental diffusion coefficients in Figure 6b, we show that segments in both PNCs are ~35% slower than they are in bulk polymer. Thus, from Figures 5 and 6, we conclude that the observed spatial and dynamic perturbation imposed by the NPs is quantitatively the same for P2VP and backbone-deuterated d3P2VP. This conclusion is also consistent with observations from the EISF presented in Figure 4.

There are two main explanations for the agreement observed in Figure 6b. First, the segmental motion in P2VP via QENS may be dominated by the more-mobile pyridine rings, so deuteration of the backbone proves inconsequential. However, we surmise that this is not the case. Agreement between temperature modulated DSC, BDS, and QENS in our previous work[11] supports the notion that QENS samples backbone reorientation in the α-process. In addition, systematic deviations of D_α in Figure 6a support the notion that backbone protons contribute in the P2VP samples. The second explanation is that the backbone and pyridine motion are highly correlated and coupled in both neat polymer and PNCs at $T >> T_g$. Not only is this explanation supported by Figure 2b, but it is well established that primary (α) and secondary (β) relaxations converge at high temperatures, such as those used in this work. Interestingly, our results imply that this coupling remains true in the presence of highly attractive NPs while segmental and chain dynamics are slowed significantly.[8,14,15]

One may reasonably expect pyridine ring relaxations to occur more easily than backbone relaxations, and therefore be decoupled in PNCs, due to their more local and less cooperative nature.[10] Furthermore, the specific interaction (hydrogen bonding) between the pyridine ring and NP surface hydroxyls may further lead to decoupling between backbone and pyridine motion in PNCs. However, these QENS measurements reveal that these effects are either weak or nonexistent in these PNCs at these high temperatures. Instead, the observed coupling between backbone and pyridine dynamics supports the conclusion that although the segmental dynamics are slowed in PNCs, the spatial relaxation and way in which the segments relax are largely unaltered from bulk.[11] This observation provides fundamental insight into the widely reported slow segmental motion in PNCs and further illuminates the microscopic dynamics that underly mechanical and transport properties in various PNC materials.

4 | CONCLUSION

We used QENS to characterize segmental dynamics in P2VP/SiO_2 PNCs comprised of fully protonated P2VP and backbone-deuterated d3P2VP. While QENS samples all protons evenly in P2VP, QENS of d3P2VP materials selectively probe the motion of the pyridine pendant group. By monitoring the mobility of segments as a function of temperature, we observed that the mobilities of the pyridine ring and backbone converge at $T > T_g$. However, in both P2VP and d3P2VP PNCs, the dynamics were reduced relative to their bulk counterparts at all temperatures. From measurements of QENS at $T >> T_g$, we observe diffusive dynamics of segments in all samples on time and length scales of ~1 ns and ~1 nm. Even though the segmental diffusion coefficient observed in d3P2VP samples (which are dominated by the pendant group) are systematically faster than P2VP samples, the normalized diffusion coefficients in 25 vol% PNCs are both ~35% slower than bulk. This observation highlights the connection between backbone and pyridine motion in P2VP-based PNCs, even when the segmental motion is temporally slowed by the attractive NPs. These results provide insight toward a fundamental and mechanistic understanding regarding the spatial and temporal impact of NPs to various molecular motions in PNCs.

ACKNOWLEDGMENTS

Eric J. Bailey and Karen I. Winey acknowledge NSF-DGE-1321851, NSF-CBET-1706014, and DOE-BES-SC0016421. Access to HFBS was provided by the CHRNS, a partnership between NIST and NSF under DMR-1508249. MAXS facility was funded in part by NSF-DMR-11-20901. Any expressed opinions, findings, and conclusions are those of the authors and do not reflect the views of NSF or NIST.

ORCID

Eric J. Bailey https://orcid.org/0000-0001-7194-9035
Karen I. Winey https://orcid.org/0000-0001-5856-3410

REFERENCES

[1] S. K. Kumar, B. C. Benicewicz, R. A. Vaia, K. I. Winey, *Macromolecules* **2017**, *50*, 714. https://doi.org/10.1021/acs.macromol.6b02330.

[2] S. Cheng, B. Carroll, V. Bocharova, J. M. Carrillo, B. G. Sumpter, A. P. Sokolov, *J. Chem. Phys.* **2017**, *146*, 203201/1. https://doi.org/10.1063/1.4978504.

[3] E. J. Bailey, K. I. Winey, *Prog. Polym. Sci.* **2020**, *105*, 101242. https://doi.org/10.1016/j.progpolymsci.2020.101242.

[4] A. C. Genix, V. Bocharova, A. Kisliuk, B. Carroll, S. Zhao, J. Oberdisse, A. P. Sokolov, *ACS Appl. Mater. Interfaces* **2018**, *10*, 33601. https://doi.org/10.1021/acsami.8b13109.

[5] Q. Chen, S. Gong, J. Moll, D. Zhao, S. K. Kumar, R. H. Colby, *ACS Macro. Lett.* **2015**, *4*, 398. https://doi.org/10.1021/acsmacrolett.5b00002.

[6] M. Jhalaria, E. Buenning, Y. Huang, M. Tyagi, R. Zorn, M. Zamponi, V. García-Sakai, J. Jestin, B. C. Benicewicz, S. K. Kumar, *Phys. Rev. Lett.* **2019**, *123*, 158003/1. https://doi.org/10.1103/PhysRevLett.123.158003.

[7] C. R. Bilchak, E. Buenning, M. Asai, K. Zhang, C. J. Durning, S. K. Kumar, Y. Huang, B. C. Benicewicz, D. W. Gidley, S. Cheng, A. P. Sokolov, M. Minelli, F. Doghieri, *Macromolecules* **2017**, *50*, 7111. https://doi.org/10.1021/acs.macromol.7b01428.

[8] A. P. Holt, P. J. Griffin, V. Bocharova, A. L. Agapov, A. E. Imel, M. D. Dadmun, J. R. Sangoro, A. P. Sokolov, *Macromolecules* **2014**, *47*, 1837. https://doi.org/10.1021/ma5000317.

[9] S. Cheng, A. P. Holt, H. Wang, F. Fan, V. Bocharova, H. Martin, T. Etampawala, B. T. White, T. Saito, N. G. Kang, M. D. Dadmun, J. W. Mays, A. P. Sokolov, *Phys. Rev. Lett.* **2016**, *116*, 38302/1. https://doi.org/10.1103/PhysRevLett.116.038302.

[10] A. P. Holt, V. Bocharova, S. Cheng, A. M. Kisliuk, G. Ehlers, E. Mamontov, V. N. Novikov, A. P. Sokolov, *Phys. Rev. Mater.* **2017**, *1*, 62601/1. https://doi.org/10.1103/PhysRevMaterials.1.062601.

[11] E. J. Bailey, P. J. Griffin, M. Tyagi, K. I. Winey, *Macromolecules* **2019**, *52*, 669. https://doi.org/10.1021/acs.macromol.8b01716.

[12] S. Gong, Q. Chen, J. F. Moll, S. K. Kumar, R. H. Colby, *ACS Macro. Lett.* **2014**, *3*, 773. https://doi.org/10.1021/mz500252f.

[13] J. Moll, S. K. Kumar, *Macromolecules* **2012**, *45*, 1131. https://doi.org/10.1021/ma202218x.

[14] E. J. Bailey, P. J. Griffin, R. J. Composto, K. I. Winey, *Macromolecules* **2020**, *53*, 2744. https://doi.org/10.1021/acs.macromol.9b02205.

[15] P. J. Griffin, V. Bocharova, L. R. Middleton, R. J. Composto, N. Clarke, K. S. Schweizer, K. I. Winey, *ACS Macro. Lett.* **2016**, *5*, 1141. https://doi.org/10.1021/acsmacrolett.6b00649.

[16] S. E. Harton, S. K. Kumar, H. Yang, T. Koga, K. Hicks, H. Lee, J. Mijovic, M. Liu, R. S. Vallery, D. W. Gidley, *Macromolecules* **2010**, *43*, 3415. https://doi.org/10.1021/ma902484d.

[17] D. N. Voylov, A. P. Holt, B. Doughty, V. Bocharova, H. M. Meyer, S. Cheng, H. Martin, M. Dadmun, A. Kisliuk, A. P. Sokolov, *ACS Macro. Lett.* **2017**, *6*, 68. https://doi.org/10.1021/acsmacrolett.6b00915.
[18] A. C. Genix, J. Oberdisse, *Curr. Opin. Colloid Interface Sci.* **2015**, *20*, 293. https://doi.org/10.1016/j.cocis.2015.10.002.
[19] J. H. Roh, M. Tyagi, T. E. Hogan, C. M. Roland, *Macromolecules* **2013**, *46*, 6667. https://doi.org/10.1021/ma401597r.
[20] A. Triolo, F. Lo Celso, F. Negroni, V. Arrighi, H. Qian, R. E. Lechner, A. Desmedt, J. Pieper, B. Frick, R. Triolo, *Appl. Phys. A: Mater. Sci. Process.* **2002**, *74*, 490. https://doi.org/10.1007/s003390201883.
[21] K. Chrissopoulou, S. H. Anastasiadis, E. P. Giannelis, B. Frick, *J. Chem. Phys.* **2007**, *127*, 144910. https://doi.org/10.1063/1.2775449.
[22] A. P. Holt, V. Bocharova, S. Cheng, A. M. Kisliuk, B. T. White, T. Saito, D. Uhrig, J. P. Mahalik, R. Kumar, A. E. Imel, T. Etampawala, H. Martin, N. Sikes, B. G. Sumpter, M. D. Dadmun, A. P. Sokolov, *ACS Nano* **2016**, *10*, 6843. https://doi.org/10.1021/acsnano.6b02501.
[23] M. Tyagi, A. Alegría, J. Colmenero, *J. Chem. Phys.* **2005**, *122*, 244909/1. https://doi.org/10.1063/1.1931664.
[24] S. Arrese-Igor, A. Arbe, B. Frick, J. Colmenero, *Macromolecules* **2011**, *44*, 3161. https://doi.org/10.1021/ma2001178.
[25] E. Senses, M. Tyagi, M. Pasco, A. Faraone, *ACS Nano* **2018**, *12*, 10807. https://doi.org/10.1021/acsnano.8b02514.
[26] J. S. Meth, S. G. Zane, C. Chi, J. D. Londono, B. A. Wood, P. Cotts, M. Keating, W. Guise, S. Weigand, *Macromolecules* **2011**, *44*, 8301. https://doi.org/10.1021/ma201714u.
[27] N. Jouault, D. Zhao, S. K. Kumar, *Macromolecules* **2014**, *47*, 5246. https://doi.org/10.1021/ma500619g.
[28] A. Meyer, R. M. Dimeo, P. M. Gehring, D. A. Neumann, *Rev. Sci. Instrum.* **2003**, *74*, 2759. https://doi.org/10.1063/1.1568557.
[29] V. F. Sears, *Neutron News.* **1992**, *3*, 26. https://doi.org/10.1080/10448639208218770.
[30] C. Ye, C. G. Wiener, M. Tyagi, D. Uhrig, S. V. Orski, C. L. Soles, B. D. Vogt, D. S. Simmons, *Macromolecules* **2015**, *48*, 801. https://doi.org/10.1021/ma501780g.
[31] P. Akcora, S. K. Kumar, V. García Sakai, Y. Li, B. C. Benicewicz, L. S. Schadler, *Macromolecules* **2010**, *43*, 8275. https://doi.org/10.1021/ma101240j.
[32] C. M. Wolf, K. H. Kanekal, Y. Y. Yimer, M. Tyagi, S. Omar-Diallo, V. Pakhnyuk, C. K. Luscombe, J. Pfaendtner, L. D. Pozzo, *Soft Matter* **2019**, *15*, 5067. https://doi.org/10.1039/c9sm00807a.
[33] T. Springer, *Quasielastic Neutron Scattering for the Investigation of Diffusive Motions in Solids and Liquids*, Springer-Verlag, Berlin, Germany **1972**.

SUPPORTING INFORMATION

Additional supporting information may be found online in the Supporting Information section at the end of this article.

How to cite this article: Bailey EJ, Tyagi M, Winey KI. Correlation between backbone and pyridine dynamics in poly(2-vinyl pyridine)/silica polymer nanocomposites. *J Polym Sci*. 2020;58: 2906–2913. https://doi.org/10.1002/pol.20200416